Electron Transfer from Plastocyanin to the Photosystem I Reaction Center in Mutants with Increased Potential of the Primary Donor in *Chlamydomonas reinhardtii*†

V. M. Ramesh,‡ Mariana Guergova-Kuras,§ Pierre Joliot,§ and Andrew N. Webber*,‡

Department of Plant Biology and Center for the Study of Early Events in Photosynthesis, P.O. Box 871601, Arizona State University, Tempe, Arizona 85287-1601, and Institut de Biologie Physico-Chimique, Centre National de la Recherche Scientifique, UPR 1261, 13 Rue Pierre et Marie Curie, 75005 Paris, France

Received July 2, 2002; Revised Manuscript Received October 8, 2002

ABSTRACT: The dependence of the P_{700}^+/P_{700} midpoint potential on kinetics of reduction of P_{700}^+ *in vivo* has been examined in a series of site-directed mutants of *Chlamydomonas reinhardtii* in which the histidyl axial ligand to the Mg^{2+} of the P_{700} chlorophyll *a* has been changed to several different amino acids. In wild-type photosystem I, the potential of P_{700}^+/P_{700} is 447 mV and the *in vivo* half-time of P_{700}^+ reduction by its natural donor, plastocyanin, is 4 μs. Substitution of the axial histidine ligand with cysteine increases the potential of P_{700}^+/P_{700} to 583 mV and changes the rate of P_{700}^+ reduction to 0.8 μs. Mutants with a range of potentials between 447 and 583 mV show a strong correlation of the P_{700}^+/P_{700} potential to the rate of reduction of P_{700}^+ by plastocyanin. There is also an increase in the rate of photosystem I-mediated electron transfer from the artificial electron donor DCPIP to methyl viologen in thylakoid membranes. The results indicate that the overall rate constant of P_{700}^+ reduction is determined by the rate of electron transfer between the copper and P_{700}^+ and confirmed that *in vivo* there is a preformed complex between plastocyanin and photosystem I. Using approximations of the Marcus electron transfer theory, it is possible to estimate that the distance between the copper of plastocyanin and P_{700}^+ is ∼15 Å. On the basis of this distance, the plastocyanin docking site should lie in a 10 Å hollow formed by the lumenal exposed loops between transmembrane helices *i* and *j* of PsaA and PsaB.

The photosynthetic electron transfer chain of cyanobacteria, algae, and plants has two photosystems that act in series to drive electron transfer from water to $NADP^+$. The photosystem I complex (PSI)[1] uses light energy to transfer electrons from plastocyanin on the lumenal side of the thylakoid membrane to ferredoxin on the stromal side of the membrane (*1*). PSI contains approximately 13 individual polypeptide subunits, some of which coordinate cofactors for light harvesting and electron transfer (*2*, *3*). The reaction center core is formed by two homologous proteins, PsaA and PsaB, each having 11 transmembrane-spanning regions. These two subunits coordinate approximately 96 Chl *a* molecules and the cofactors that participate in the initial electron transfer (*4*). The structure of PSI (*5*) showed that the five C-terminal transmembrane helices of both subunits coordinate the cofactors that transfer electrons from the lumenal side to the stromal side of PSI. The two terminal electron acceptors F_A and F_B (4Fe−4S clusters) are coordinated by the PsaC subunit. Light energy absorbed by the antenna chlorophylls is transferred to P_{700} where charge separation occurs between P_{700}^+ (a Chl *a*−Chl *a*′ dimer) and A_0^- (a Chl *a* monomer). Electrons are then transferred sequentially from A_0 to A_1 (a phylloquinone), F_X (another 4Fe−4S cluster), F_A and F_B, and finally to the soluble acceptor ferredoxin. Two symmetrical pigment branches each forming a potential pathway for electron transfer from P_{700} to F_X were revealed by the X-ray structure (*5*), and there is some evidence that both branches participate in electron transfer (*6*, *7*).

Reduction of P_{700}^+ by plastocyanin, a small Cu-containing protein, occurs at the lumenal side of the thylakoid membrane. This reaction has been investigated in detail in *Chlamydomonas* and other model systems. In vitro, electron transfer is biphasic with a fast first-order rate constant of 3−12 μs, representing electron transfer within a preformed complex (*8*, *9*), and a variable slower second-order reaction limited by the docking of plastocyanin to PSI (*10*). In intact chloroplasts (*8*, *9*) and whole cells of green algae (*12*), only the fast, first-order phase has been observed, showing that the *in vivo* electron transfer in these systems occurs from a preformed complex between plastocyanin and PSI. Mutagenesis studies showed that both PsaF (*13*) and its interaction with PsaJ (*14*) are important for forming a transient complex between the soluble donor and the PSI complex. In the

† This work was supported by the National Research Initiatives Competitive Grants Program of the U.S. Department of Agriculture (2001-35318-11137).

* To whom correspondence should be addressed: Department of Plant Biology, P.O. Box 871601, Arizona State University, Tempe, AZ 85287-1601. Phone: (480) 965-8725. Fax: (480) 965-6899. E-mail: andrew.webber@asu.edu.

‡ Arizona State University.

§ UPR 1261.

[1] Abbreviations: Chl *a*, chlorophyll *a*; DCPIP, 2,6-dichlorophenolindolphenol; ENDOR, electron nuclear double resonance; MV, methyl viologen; PSI, photosystem I; P_{700}, primary electron donor in PSI.

10.1021/bi026392z CCC: $22.00 © 2002 American Chemical Society
Published on Web 11/20/2002

absence of structural information from cocrystals, the precise docking site for plastocyanin on PSI remains unknown. A 10 Å hollow on the lumenal side of PSI formed by the lumen-exposed loops connecting transmembrane helices *i* and *j* of PsaA and PsaB has been hypothesized as a possible plastocyanin binding site (*5*).

The pathway of electron transfer from the soluble electron donor will strongly depend on the electronic structure of P_{700}^+. In the ground state, P_{700} is clearly a dimer of excitonically coupled Chl *a* molecules (*4*). However, the electronic structure of P_{700}^+ is less well understood. On the basis of the results of ENDOR and ESEEM experiments with frozen solution and crystals of PSI, it has been shown that the electron spin distribution over the two Chls of P_{700}^+ is highly asymmetric, ranging from 3:1 to 10:1 (*15*−*19*). A detailed analysis of isotopically labeled P_{700} suggested the complete localization of the unpaired electron on a single Chl (*20*). In *Chlamydomonas*, the axial ligands to P_{700}, His676 of PsaA and His656 of PsaB, have been mutated to a range of hydrophobic and hydrophilic amino acids (*21*−*23*). These mutants have been analyzed to determine how they affect the spectroscopic properties of PSI, and in particular to determine the directionality of asymmetry of the unpaired electron in P_{700}^+ (*19*, *21*, *22*). Mutation of His656 of PsaB has several effects on P_{700}^+, including an increase in the midpoint potential of P_{700}^+/P_{700}, a changed absorption difference spectra, and a modified ^{1}H ENDOR spectrum (*21*, *22*). However, analogous mutations of the symmetric histidine ligand on PsaA resulted in only a modest change in the midpoint potential and the ^{1}H ENDOR spectra of P_{700}^+/P_{700} (*22*). These results indicated that the electron spin density in P_{700}^+ is located on the PsaB side chlorophyll molecule, consistent with the recently identified H-bonding pattern of the P_{700} dimer (*5*). Thus, electron transfer from plastocyanin to P_{700}^+ needs to be considered on the basis of the distance between the Cu of plastocyanin and the Chl *a* on the PsaB side of P_{700}^+.

To better understand the nature of electron donation to P_{700}^+, we have investigated how the rate of electron transfer to the reaction center is dependent upon the driving force, i.e., the free energy difference between the electron donor and acceptor. Recently, a series of PSI mutants have been designed that alter the midpoint potential of the PSI primary donor in the range from 447 (wild type) to 583 mV (*21*, *22*). In this paper, we show that there is strong correlation between the P_{700}^+/P_{700} potential and the rate of reduction of P_{700}^+ by artificial donors and plastocyanin. The results confirm that, *in vivo*, electron transfer occurs within a preformed complex, and further allow an estimation of the distance between the Cu^{2+} of plastocyanin and P_{700}^+ that sets constraints for the location of the plastocyanin binding site on PSI.

MATERIALS AND METHODS

Generation and Propagation of PSI Mutants. Site-directed mutagenesis was used to introduce specific mutations into the *psaA* and *psaB* genes using protocols essentially as described previously (*21*, *24*). The *Chlamydomonas reinhardtii* recipient strains for transformation were CC125 (wild-type *mt*$^+$) and a mutant strain, CC2696, that lacks Chl *b* and PSII, both obtained from the *Chlamydomonas* Culture Collection at Duke University (Durham, NC). Chloroplast transformation was performed by the biolistics technique as previously described (*25*, *26*). Bombarded cells were transferred to plates containing CC medium (*24*) supplemented with 100 μg/mL spectinomycin and 1.2% agar and placed under dim light for 14 days until colonies appeared. Single transformant colonies were restreaked onto solid medium. Total DNA was isolated from cells taken from confluent regions of the plates as previously described (*26*) and resuspended at a final volume of 100 μL. One microliter of this DNA isolation was then used as a template for PCR to confirm the introduction or loss of a specific restriction enzyme site. To confirm the presence of the desired mutation, the amplified DNA from the homoplasmic strains was sequenced.

Strains CC125 and CC2696 and their transformants were maintained on agar plates with acetate-containing CC medium (*24*). For thylakoid membrane preparations, cells were grown in CC liquid medium to a density of $1-1.5 \times 10^{-6}$ cells/mL at a light intensity of 50 mmol m^{-2} s^{-1}. Growth tests were initiated by spotting 15 μL of log-phase cultures onto agar plates. Anaerobiosis was established using the BioMerieux (Marcy, Etiole, France) Generbag Anaer system according to the manufacturer's instructions using a gas supply of 90% N_2, 5% CO_2, and 5% H_2.

Isolation of Thylakoid Membranes and Protein Analysis. Thylakoid membranes were isolated from wild-type and mutant cells according to the method described in ref *27*. To determine the steady state level of PSI in *Chlamydomonas* cells, thylakoid membranes were solubilized in gel loading buffer [5% lithium dodecyl sulfate, 100 mM dithiothreitol, 10% glycerol, and 50 mM Tris (pH 8.8)] and the Chl−protein complexes separated by LDS−PAGE at 4 °C. Following electrophoresis, the PSI complexes were either visualized as a green band at the top of the gel or stained with Coomassie blue (*28*). Gels were loaded on a constant chlorophyll basis. Densitometry gel scanning of Coomassie-stained samples was performed using a GDS-8000 system (UVP Bioimaging system). A series dilution of wild-type membranes (Figure 1) was scanned. The level of PSI was linearly correlated with the density of the stained band ($R^2 = 0.9558$) (not shown).

Electron Transport Measurements in Vitro. PSI activity was measured polarographically as light-induced oxygen uptake in the presence of methyl viologen (2 mM), 2,6-dichlorophenolindolphenol (1 mM), ascorbate (5 mM), 3-(3,4-dichlorophenyl)-1,1-dimethylurea (50 μM), and sodium azide (5 mM) in 40 mM HEPES buffer (pH 7.2).

Optical Spectroscopy in Vivo. Spectroscopic measurements on whole cells of *Chlamydomonas* were performed by using a spectrophotometer where absorption changes were probed by using short monochromatic flashes, as described previously (*6*, *7*). In the spectral range of 425−500 nm, the pulses were produced by a Quanta-Ray MOPO-710 (Spectra-Physics) Nd:Yag pumped optical parametric oscillator and in the range of 375−430 nm by an FDO-900 frequency doubler accessory device (Spectra-Physics). The sample was excited at 700 nm by a tunable dye laser pumped by the second harmonic of a Nd:Yag laser. *Chlamydomonas* cells were grown in Tris-acetate-phosphate medium (*7*) at 25 °C under low light (6 μmol m^{-2} s^{-1}). For spectroscopic measurements, the cells were resuspended in 20 mM Hepes

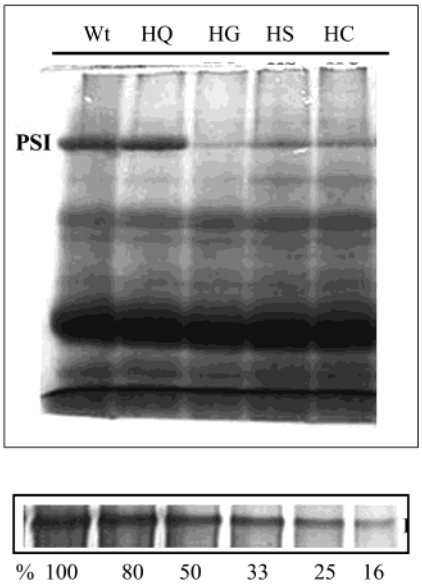

FIGURE 1: Accumulation of PSI in thylakoid membranes of the wild type and transformants. Membrane protein complexes were resolved by nondenaturing LDS−PAGE and stained with Coomassie brilliant blue. The bottom panel shows a dilution series of wild-type membranes.

Table 1: Growth Characteristics of PsaA and PsaB Mutants

	aerobic low light	aerobic high light	anaerobic high light
wild type (CC125)	+	+++	++
HQ(B656)	+	++	++
HS(B656)	+	±	++
HC(B656)	+	+	++
HG(B656)	+	+	++

(pH 7.2) containing 20% (w/v) Ficoll, as well as 5 μM FCCP to collapse the permanent transmembrane potential. The dependence of the flash-induced absorption changes at 430 and 380 nm upon the energy of the actinic flash was measured for each strain. Kinetics measurements were performed with light energies just sufficient to saturate the signal at 380 nm. The decay-associated spectra of the kinetic phases were obtained from a global analysis of the individual kinetics obtained at each wavelength, using the MEXFIT program (*29*).

RESULTS

Growth Characteristics. To determine how the individual mutations alter the growth characteristics of the cells, we performed spot tests of the growth of the wild type and transformants under phototrophic and heterotrophic conditions (Table 1). All of the transformants derived from CC125 could grow heterotrophically, or phototrophically under anaerobic conditions. However, under phototrophic growth at high light, the HS(B656), HG(B656), and HC(B656) mutants grow slower. The impaired growth of the mutants correlated qualitatively with the reduced level of PSI in these mutants (below). Functional complementation of each of the mutants with the wild-type gene always restored normal growth phenotypes, indicating that the site-directed modification was the cause of the observed phenotype, and that no other mutation was introduced during the mutagenesis procedure.

Table 2: Accumulation and Electron Transfer of PSI in Isolated Thylakoids

	P_{700} midpoint potential[a] (mV)	relative PSI e^- transfer rate[b] (%) ($n = 4$)	relative PSI amount (%)[c] ($n = 4$)	PSI e^- transfer rate/P_{700} (%)
wild type	447	100	100	100
HQ(B656)	465	214 ± 6	92 ± 2	232
HS(B656)	480	216 ± 6	39 ± 1	553
HG(B656)	545	223 ± 5	13 ± 1	1715
HC(B656)	587	364 ± 8	31 ± 2	1174

[a] From refs *21* and *22*. [b] DCPIP to MV. [c] From nondenaturing gels.

Accumulation of Photosystem I. The steady state level of PSI in *Chlamydomonas* cells was determined by nondenaturing LDS−PAGE. Thylakoid membranes were isolated from wild-type and transformant cells and the Chl−protein complexes separated by LDS−PAGE at 4 °C. The PSI complex can be clearly visualized as a green band near the top of the gel, which can also be stained with Coomassie blue. This approach was more sensitive than spectroscopic methods for determining PSI levels in mutant thylakoids with reduced PSI content. As shown in Figure 1, PSI in the mutants accumulated to a level that was significantly lower than in wild-type cells. Accurate comparison of the relative amounts of the PSI complex was achieved by densitometric scanning of the Coomassie-stained nondenaturing gel (Table 2), using the dilution series shown in Figure 1. The HQ(B656) mutation was the least disruptive and resulted in little change in the PSI level. The HS(B656), HG(B656), and HC(B656) mutants accumulated to levels that were ~10−50% of the wild-type level (Table 2).

Photosystem I Activity in Thylakoids. To examine the effect of the mutations on PSI electron transport, thylakoids were isolated from the mutant and wild-type cells and PSI-mediated light-induced electron transfer from DCPIP to methyl viologen was assessed by measuring the extent of oxygen uptake. As previously reported, very low levels of light-induced oxygen uptake by methyl viologen are obtained even in the absence of PSI activity (*30*). Therefore, we determined the rate of light-induced oxygen uptake from thylakoids isolated from CC2341 cells that lack PSI, and subtracted that value from the rate of light-induced oxygen uptake obtained from the mutant thylakoid membranes. Each mutant showed electron transfer rates that were higher than that of the wild type, despite the reduced level of accumulation of PSI in the membranes (Table 2).

The last column in Table 2 shows the rate of PSI electron transfer normalized to the relative amount of PSI present in the membranes. Again, all mutants show an increase in the rate of electron transfer. The HQ(B656), HS(B656), and HC(B656) mutants show rates that are ~3, 4, and 8 times faster, respectively, than that of the wild type.

Optical Spectroscopy. Using transient absorption spectroscopy, it was possible to measure the rate of reduction of P_{700}^+ by plastocyanin in whole cells. To improve the signal, these experiments were performed in strain CC2696 that lacked both PSII and the peripheral, Chl *b*-containing antenna complex (*31*). The CC2696 strain has not previously been characterized, so transient absorption signals in the nanosecond to microsecond time scale were recorded at discrete wavelengths in the spectral range of 370−500 nm after

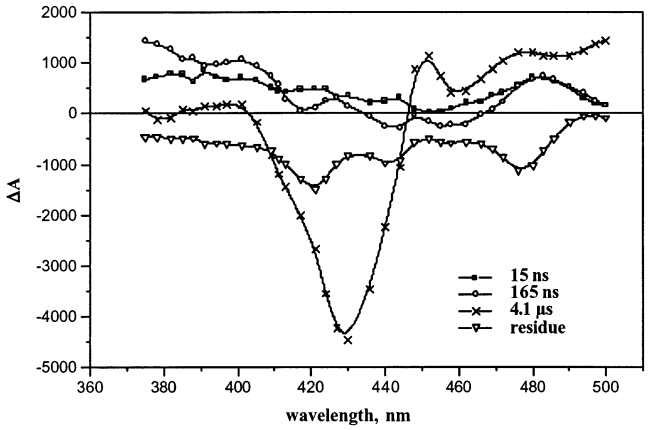

FIGURE 2: Deconvolution of the spectra for the three kinetic components in whole cells of *C. reinhardtii* CC2696. The values, expressed as half-times, are deduced from fitting three exponential components to the kinetic data over all the wavelengths, and the assignment is as follows: 15 and 165 ns, fast and slow phases of phylloquinone reoxidation, respectively; and 4 μs, P_{700}^+ reduction by plastocyanin; and residue, the absorption that does not decay over the time scale used in the experiment (30 μs).

selective laser flash excitation (700 nm) of PSI. Global analysis of the kinetics data (Figure 2) resolved four components: three exponential decays (two in the nanosecond and one in the microsecond time range) and a residue component that did not decay on the detection time scale (30 s), as previously observed with *Chlamydomonas* strains (*7*). The spectrum of the nondecaying component was associated with the electrochromic shifts due to the flash-induced delocalized membrane potential (*7*). The spectra of the two nanosecond phases were attributed to reoxidation of two reduced phylloquinones (*6*, *7*). The microsecond component was assigned to P_{700}^+ reduction, based on the typical bleaching at 430 nm (*32*) and a half-time of 4 μs characteristic of its reduction by plastocyanin in intact algae (*12*).

From the reference strain CC2696, the mutant strains with modified midpoint potentials of P_{700}^+/P_{700} were obtained by transformation as described in Materials and Methods. The kinetics of P_{700}^+ reduction were studied in whole cells of those mutants using the decay of the bleaching at 430 nm obtained with a subsaturating excitation (Figure 3). The kinetics in the mutant strains are clearly faster than in the WT. However, they could be well fit by a single exponential. This would suggest that the electron transfer is still performed within a preformed complex (*8*, *9*) and the mutations do not alter the docking of the PC to PSI. The rate constant of the electron transfer is however dependent on the redox potential of P_{700}/P_{700}^+. Increasing the P_{700}/P_{700}^+ potential by 136 mV in the HC(B656) mutant leads to a rate in this mutant that is 5 times faster (Table 2).

The effect of the modified axial ligand on the spectrum of P_{700}^+ was studied for the HG(B656) mutant (Figure 4). The spectrum associated with the microsecond reduction of P_{700}^+ for the mutant (panel B) is compared to that of the reference strain CC2696 (panel A). Although both spectra are quite similar in overall shape, a decrease in the intensity of the main peak at 430 nm in favor of the intensity of the shoulder at 412 nm can be noticed in the mutant strain.

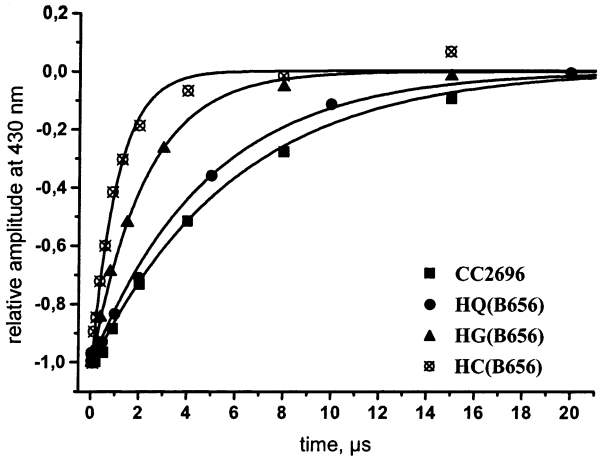

FIGURE 3: Kinetics of P_{700}^+ re-reduction by plastocyanin in whole cells of *C. reinhardtii*. Data are shown as filled symbols, and the best exponential fits with parameters shown in Table 3 are shown as lines. Kinetics were taken at 430 nm, and the signal was normalized to the maximum negative absorbance at 0.05 μs.

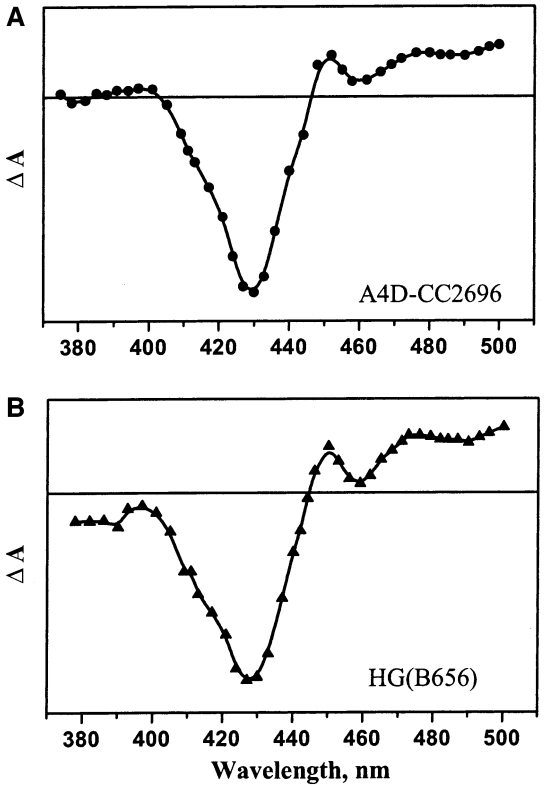

FIGURE 4: Spectra associated with P_{700}^+ reduction in the HG(B656) (B) and CC2696 (A) strains. Decay-associated spectra were obtained from a global deconvolution of kinetic data measured in whole cells (see the text for more details). The decay half-times associated with the spectra are 4.1 μs for the CC2696 strain and 1.6 μs for the HG(B656) strain.

DISCUSSION

In this work, we have examined how the midpoint potential of P_{700}^+/P_{700} can modulate the electron transfer from its donor. We showed that increasing the potential of P_{700}^+/P_{700} and therefore the driving force for electron transfer between the soluble donor and PSI induces an increase in the rate of re-reduction of P_{700}^+. As the potential of P_{700}^+/P_{700} was increased from 440 mV in the wild type to 583 mV in the HC(B656) mutant, the characteristic half-time for P_{700}^+

reduction by plastocyanin was decreased from 4 to 0.8 μs. A similar increase in the rate of PSI electron transfer from the artificial donor, DCPIP, to MV was also observed. Since DCPIP is a slow donor, this result was expected, as the overall rate of electron transfer through PSI to MV would depend on the amount of PSI present in the membrane and also on the difference in the potentials of the donor and acceptor. However, the rate of electron transfer will also be dependent upon diffusion of DCPIP to its site of electron donation (i.e., the accessibility of DCPIP to P_{700}), so it is not valid to attempt to directly correlate changes in the midpoint potential of P_{700} with rates of electron transfer from DCPIP to MV. Replacement of the axial ligands of P_{700} in *Chlamydomonas* also resulted in significant alteration in phenotype growth and PSI accumulation. Substitution of His656 of PsaB with large hydrophobic residues has been shown previously to result in little or no accumulation of PSI (*23*, *33*). Substitution of PsaB His656 with amino acids with N-containing side chains allowed for substantial accumulation of PSI, as might be expected with such conservative substitutions. However, replacement of His with Ser resulted in a 50−60% loss of PSI, indicating some moderate change in either the assembly or stability. Replacement of His656 with Gly or Cys resulted in an ~60% loss of PSI. These mutants also showed a reduced growth capability under high light, which is probably related to the decreased PSI content. It has been well documented that impaired electron donation to PSI results in increased light sensitivity (*34*). This has been studied primarily in site-directed or null mutants of *psaF*, which show impaired interaction between plastocyanin and PSI. While the mutants studied here all show an increased rate of electron donation to PSI, it is probably not sufficient to compensate for the decreased level of PSI and the resulting imbalance of electron flow through PSII and PSI.

In wild-type cells and each of the mutants, the reduction of P_{700}^+ by plastocyanin is a first-order reaction fit well by a single-exponential component. This indicates that the electron transfer reactions in the mutants occur within a preformed complex of plastocyanin and PSI. It also suggests that the overall rate is limited by the distance between the copper and the chlorophyll dimer of PSI. This supports previous suggestions based on work using intact chloroplasts (*8*, *11*) and algae (*12*), which indicate that plastocyanin forms a stable complex with PSI prior to electron transfer. This also indicates that the mutations have not altered the binding affinity of the reaction center for plastocyanin in a manner that significantly effects the electron transfer reaction. This is perhaps expected as the sites of the mutations are the axial ligands of the P_{700} Chls that are buried within the protein, and not a part of the surface exposed to the lumen where binding of the plastocyanin is expected to occur.

Conventional electron transfer theory indicates that the rate of electron transfer has an exponential dependence upon the free energy difference for the reaction. In the case of electron transfer from plastocyanin to P_{700}^+, the free energy difference between the initial state, PC^+/P_{700}^+, and the final state, PC^{2+}/P_{700}, is determined by the relative difference in the oxidation/reduction midpoint potentials. For wild-type PSI, the midpoint potential of P_{700}/P_{700}^+ is 447 mV (*21*) and 370 mV for plastocyanin, so the free energy difference is −77 meV (Table 3). Although these values have been measured *in vitro* and not adjusted for possible changes in the potentials due to formation of the complex (*9*), the differences would presumably be similar for each mutant and so would not effect the basic interpretation of the results.

Table 3: Electron Transfer Kinetics between Plastocyanin and PSI in *Chlamydomonas* Mutants

	Em(P_{700}^+/P_{700}) (mV)[a]	ΔG (meV)[b]	$t_{1/2}$ (μs)[c]	log(k_{et}) (s^{-1})
wild type	447	−77	4	5.23
HQ(B656)	465	−95	3.3	5.32
HS(B656)	480	−110	2	5.54
HG(B656)	545	−175	1.5	5.66
HC(B656)	583	−213	0.8	5.96

[a] The values for the Em of P_{700}^+/P_{700} were taken from refs *21* and *22*. [b] ΔG is obtained as the difference between the midpoint potentials of the electron donor (plastocynin, 370 mV) and the electron acceptor (P_{700}^+) in the different mutant strains. [c] The half-time of P_{700}^+ reduction is obtained by fitting a one-exponential decay to the kinetics at 430 nm (Figure 3).

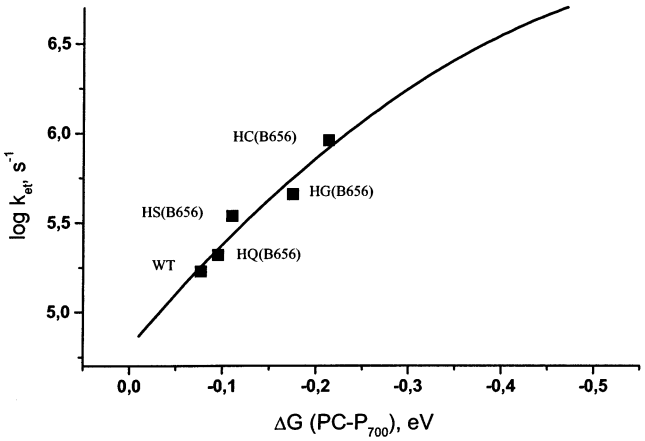

FIGURE 5: Relationship of the rate constant of P_{700}^+ reduction to the free energy change in different mutants. See the text for details.

The relationship between the rate of electron transfer, k, and $\Delta G°$ can be modeled using conventional Marcus electron transfer theory (*35*) according to

$$k = (4\pi^2/h)V^2(4\pi\lambda k_B T)^{-1/2} \times \exp[(-\Delta G° + \lambda)^2/(4\lambda k_B T)] \quad (1)$$

where h is Planck's constant, V is the electronic coupling factor between the initial and final states, k_B is the Boltzmann constant, T is the temperature, and λ is the reorganization energy. The data are fit well to eq 1 using a λ value of 545 meV (Figure 5), but because of the narrow range of $\Delta G°$ values, this value for λ is only a lower estimate. However, a similar reorganization energy (~500 meV) has already been observed for another interprotein donor−acceptor system in which the electron donor (cyt c_2) forms a complex with the electron acceptor (RC of purple bacteria) prior to electron transfer (*36*). Our fit predicts a maximum rate of 2.62×10^6 s^{-1} when the free energy difference equals λ. The results demonstrate that the observed rate for electron transfer from plastocyanin to P_{700}^+ is significantly slower than the optimal rate since the driving force is far less than the reorganization energy. In PSI, only the Chl a' of the P_{700} dimer is H-bonded by the PsaA (*5*). Additional H-bonding to the Chl a by PsaB could potentially increase the potential of P_{700}^+/P_{700} and thus

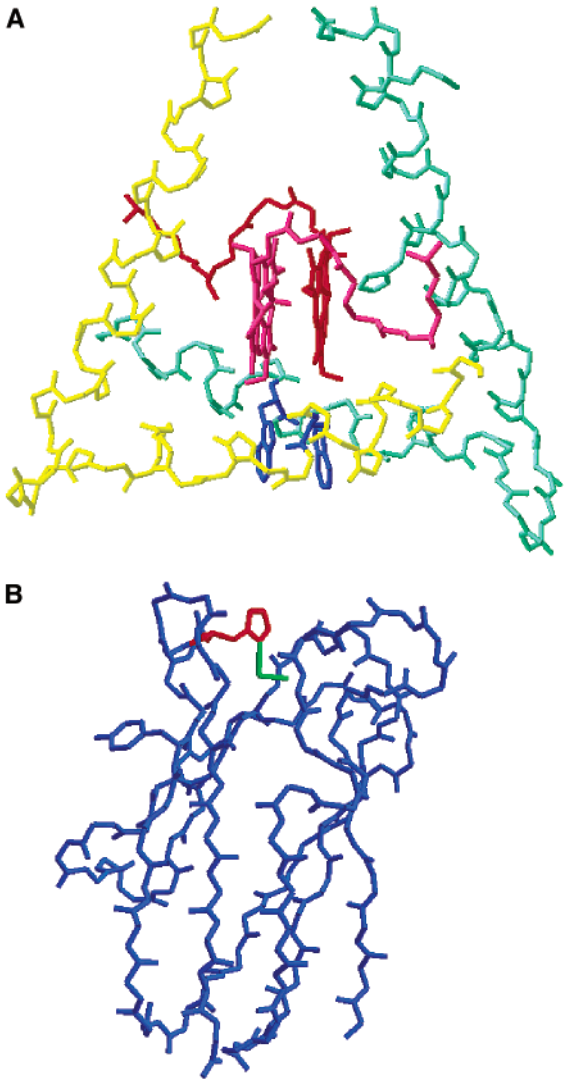

FIGURE 6: (A) Model of the plastocyanin docking domain formed by the *i*−*j* loops of PsaA (yellow) and PsaB (green). Conserved Trp residues that may serve to mediate electron transfer are shown in blue. The distance from the edge of the chl of P_{700}^+ (PsaB-side Chl) to the edge of the Trp of PsaA or PsaB is 10.4 or 9.6 Å, respectively. (B) Model of plastocyanin showing the Cu (green) and conserved surface His87 (red). The acidic east face that interacts with PsaF is on the left. The distance from the Cu to the edge of His87 is 4.5 Å.

lead to a faster rate, but it is unlikely that this would increase the potential by more than 50 mV (*37*). However, the rate of electron transfer from plastocyanin to P_{700}^+ is already significantly faster than the 30 ms rate of charge recombination from F_A/F_B or the 1 ms rate from F_X. Thus, any increase in the rate of electron transfer from plastocyanin would not significantly improve the quantum efficiency of PSI electron transfer, so there has probably been no significant evolutionary pressure to maximize the rate of electron transfer.

According to Dutton's model for electron transfer in proteins (*38*, *39*), the maximal rate of electron transfer is determined by the edge-to-edge distance between the cofactors of the electron donor and acceptor and an empirical factor that depends on the packing density of the intraprotein space that separates them. Using this approximation and an average packing density of 0.8, we can predict that the distance between the Cu atom of plastocyanin and the edge of P_{700}^+ would be ∼15 Å. The pathway of electron transfer from Cu to the surface of plastocyanin is well established. Site-directed mutagenesis showed that a surface-exposed histidine (His87 in many species) participates in the electron transfer from the Cu (*11*). The distance from the Cu to the edge of His87 is ∼4.5 Å based on the three-dimensional structures of plastocyanin. On the basis of mutagenesis studies, it has been shown that the Chl *a* ligated by the PsaB subunit carries most of the positive charge of P_{700}^+ (*21*, *22*). Inspection of the recent 2.5 Å structure indicates that the surface loop regions between helices *i* and *j* of PsaA and PsaB are approximately 10 Å from the P_{700} Chl (Figure 6). The plastocyanin must dock to PSI so that His87 is in contact with the *i*−*j* region of PSI, yielding a total distance of ∼15 Å between the two cofactors. This position is also in good agreement with earlier docking predictions (*40*). A close inspection of the surface-exposed *i*−*j* loops of PsaA and PsaB showed conserved Trp residues (Figure 6 and ref *41*). Indeed, mutation of the B-side tryptophan was recently shown to result in PSI complexes that lack the fast phase of electron transfer from P_{700} to PSI (*41*). The distance between the edge of the P_{700}^+ Chl and the surface edge of the Trp is ∼9.6 Å for the PsaB-side Trp and 10.4 Å for the PsaA-side Trp. Our results can account for both distances; however, the packing density between PSI and the PC would be slightly different in the two cases. If PsaA Trp is used, our results predict a packing density of 0.77, whereas the packing density would be 0.71 if the PsaB Trp were used. Since the packing density between the two centers will largely depend on the docking of the plastocyanin to PSI, further computer modeling of the docking site and/or specific mutagenesis of both tryptophan residues is needed to provide more information about the precise pathway of electron transfer between the two proteins.

REFERENCES

1. Brettel, K., and Liebl, W. (2001) *Biochim. Biophys. Acta 1507*, 100−114.
2. Webber, A. N., and Bingham, S. E. (1998) in *Molecular Biology of Chlamydomonas: Chloroplasts and Mitochondria* (Rochaix, J. D., Merchant, S., and Goldschmidt-Clermont, M., Eds.) pp 323−348, Kluwer Academic Publishers, Dordrecht, The Netherlands.
3. Scheller, H. V., Jensen, P. E., Haldrup, A., Lunde, C., and Knoetzel, J. (2001) *Biochim. Biophys. Acta 1507*, 41−60.
4. Fromme, P., Jordan, P., and Krauss, N. (2001) *Biochim. Biophys. Acta 1507*, 5−31.
5. Jordan, P., Fromme, P., Klukas, O., Witt, H. T., Saenger, W., and Krauss, N. (2001) *Nature 411*, 909−917.
6. Joliot, P., and Joliot, A. (1999) *Biochemistry 38*, 11130−11136.
7. Guergova-Kuras, M., Boudreaux, B., Joliot, A., Joliot, P., and Redding, K. (2001) *Proc. Natl. Acad. Sci. U.S.A. 98*, 4437−4442.
8. Bottin, H., and Mathis, P. (1985) *Biochemistry 24*, 6453−6460.
9. Hippler, M., Drepper, F., Farah, J., and Rochaix, J. D. (1997) *Biochemistry 36*, 6343−6349.
10. Drepper, F., Hippler, M., Nitscke, W., and Haehnel, W. (1996) *Biochemistry 35*, 1282−1295.
11. Haehnel, W., Ratajczak, R., and Robenek, H. (1989) *J. Cell Biol. 108*, 1397−1405.
12. Delosme, R. (1991) *Photosynth. Res. 29*, 45−54.
13. Farah, J., Rappaport, F., Choquet, Y., Joliot, P., and Rochaix, J. D. (1995) *EMBO J. 14*, 4976−4984.
14. Fischer, N., Boudreau, E., Hippler, M., Drepper, F., Haehnel, W., and Rochaix, J. D. (1999) *Biochemistry 38*, 5546−5552.
15. Davis, I. H., Heathcote, P., MacLachlan, D. J., and Evans, M. C. W. (1993) *Biochim. Biophys. Acta 1143*, 183−189.
16. Rigby, S. E. J., Nugent, J. H. A., and O'Malley, P. J. (1994) *Biochemistry 33*, 10043−10050.
17. Käss, H., Fromme, P., and Lubitz, W. (1996) *Chem. Phys. Lett. 257*, 197−206.

18. Käss, H., Fromme, P., Witt, H. T., and Lubitz, W. (2001) *J. Phys. Chem. B 105*, 1225−1239.
19. Webber, A. N., and Lubitz, W. (2001) *Biochim. Biophys. Acta 157*, 61−79.
20. Mac, M., Bowlby, N. R., Babcock, G. T., and McCracken, J. (1998) *J. Am. Chem. Soc. 120*, 13215−13223.
21. Webber, A. N., Su, H., Bingham, S. E., Käss, H., Krabben, L., Kuhn, M., Jordan, R., Schlodder, E., and Lubitz, W. (1996) *Biochemistry 35*, 12857−12863.
22. Krabben, L., Schlodder, E., Jordan, R., Carbonera, D., Giacometti, G., Lee, H., Webber, A. N., and Lubitz W. (2000) *Biochemistry 39*, 13012−13025.
23. Redding, K., MacMillan, F., Leibl, W., Brettl, K., Hahnley, J., Rutherford, A. W., Breton, J., and Rochaix, J.-D. (1998) *EMBO J. 17*, 50−60.
24. Lee, H., Bingham, S. E., and Webber, A. N. (1998) in *Methods in Enzymology*, Vol. 297, pp 311−319, Academic Press, Orlando, FL.
25. Boynton, J. E., Gillham, N. W., Harris, E. H., Hosler, J. P., Johnson, A. M., Jones, A. R., Randolph-Anderson, B. L., Robertson, D., Klein, T. M., Shark, K. B., and Sanford, J. C. (1988) *Science 240*, 1534−1538.
26. Webber, A. N., Gibbs, P. B., Ward, J. B., and Bingham, S. E. (1993) *J. Biol. Chem. 268*, 12990−12995.
27. Chua, N. H., and Bennoun, P. (1975) *Proc. Natl. Acad. Sci. U.S.A. 72*, 2175−2179.
28. Cui, L., Bingham, S. E., Kuhn, M., Käss, H., Lubitz, W., and Webber, A. N. (1995) *Biochemistry 34*, 1549−1558.
29. Müller, K.-H., and Plesner, P. (1991) *Eur. Biophys. J. 19*, 231−240.
30. Fujii, T., Yokoyama, E.-I., Inoue, K., and Saurai, H. (1990) *Biochim. Biophys. Acta 1015*, 41−48.
31. Werst, M., Jia, Y. W., Mets, L., and Fleming, G. R. (1992) *Biophys. J. 61*, 868−878.
32. Ke, B. (1972) *Arch. Biochem. Biophys. 152*, 70−77.
33. Melkorzernov, A. N., Su, H., Webber, A. N., and Blankenship, R. E. (1998) *Photosynth. Res. 56*, 197−207.
34. Hippler, M., Biehler, K., Krieger-Liszkay, A., van Dillewjin, J., and Rochaix, J.-D. (2000) *J. Biol. Chem. 275*, 5852−5859.
35. Marcus, R. A., and Sutin, N. (1985) *Biochim. Biophys. Acta 811*, 265−322.
36. Lin, X., Williams, J. C., Allen, J. P., and Mathis, P. (1994) *Biochemistry 33*, 13517−13523.
37. Williams, J. C., Alden, R. G., Murchison, H. A., Peloquin, J. M., Woodbury, N. W., and Allen, J. P. (1992) *Biochemistry 31*, 11029−11037.
38. Moser, C. C., Keske, J. M., Warncke, K., Farid, R. S., and Dutton, P. L. (1992) *Nature 355*, 796−802.
39. Page, C. C., Moser, C. C., Chen, X. X., and Dutton, P. L. (1999) *Nature 400*, 47−52.
40. Fromme, P., Schubert, W. D., and Krauss, N. (1994) *Biochim. Biophys. Acta 1187*, 99−105.
41. Sommer, F., Drepper, F., and Hippler, M. (2002) *J. Biol. Chem. 277*, 6579−6581.

BI026392Z